Rare Metal Materials and Engineering
Volume 52, Issue 1, January 2023
Available online at www.rmme.ac.cn

Science Press

Cite this article as: Liu Xi, Deng Binbin, Li Chuanqiang. Effect of Annealing Twins on Corrosion Resistance of hcp Binary Mg-Li Alloy[J]. Rare Metal Materials and Engineering, 2023, 52(01): 95-102.

ARTICLE

Effect of Annealing Twins on Corrosion Resistance of hcp Binary Mg-Li Alloy

Liu Xi, Deng Binbin, Li Chuanqiang

School of Materials and Energy, Guangdong University of Technology, Guangzhou 510006, China

Abstract: Corrosion resistance of as-extruded and as-annealed binary Mg-*x*Li (*x*=1, 3, 5, wt%) alloys was investigated via immersion tests, electrochemical tests, corrosion morphology observation, and scanning Kelvin probe tests. Results reveal that the annealing twins form in the as-extruded alloys after annealing at 350 °C for 4 h, and the corrosion resistance of the as-annealed alloys is obviously worse than that of as-extruded alloys in 0.1 mol/L NaCl solution. Typical filiform corrosion appears in as-extruded alloys at the initial corrosion stage, according to the analysis results of scanning electron microscope and laser confocal 3D morphology observation. Some corrosion pits are gradually formed with prolonging the corrosion duration. The rapid corrosion damage occurs on the as-annealed alloy surface, and meanwhile the relatively large and deep corrosion pits appear on the alloy surface. Besides, the distribution of isopotential line of corrosion indicates the occurrence of preferential corrosive degradation in the annealing twin areas. Thus, the micro-galvanic effect is formed between the annealing twins and parental grains with annealing twins as anode and parental grains as cathode, which decreases the corrosion resistance of as-annealed Mg-Li alloys.

Key words: Mg-Li alloy; annealing twins; corrosion; electrochemical; micro-galvanic

Mg-Li alloys have great potential as structural material in automobile and aerospace industries due to their lightweight, low density, and high specific strength and stiffness[1–4]. However, the poor mechanical strength and inferior corrosion resistance restrict their applications[5–8]. Plastic processing (extrusion, rolling, forging) is a common approach to improve the mechanical properties of magnesium alloys[6,9–11]. For the Mg alloys, twinning is an important deformation mode to accommodate the strain, due to the limited independent slip systems of hexagonal close-packed (hcp) crystal structure[12]. Although the decreased *c*/*a* ratio can facilitate the slip of non-basal planes due to the lithium addition, Mg-Li alloys still have the hcp structure when the lithium content is less than 5.5wt%[13]. Therefore, the twins can form easily in Mg-Li alloys during plastic deformation. The modified microstructure caused by plastic deformation can affect the corrosion resistance of alloy, and the effect of deformation twins on the corrosion behavior of traditional Mg alloys has been studied in recent years[14–18].

Different theories are proposed to explain the effect of twins. One is that the twins can retard the corrosion of Mg alloys, while another is that the twins can accelerate the deterioration due to the micro-galvanic corrosion[14,16–17]. Zou et al[14] reported that the extension twinning accelerates the oxide film formation, resulting in improved corrosion resistance of Mg-Y alloys. Liu et al[15] demonstrated that the micro-galvanic effect plays dual roles. The twins decrease the corrosion resistance at the initial stage. However, after corrosion for a long time, a film forms on the matrix surface, which improves the corrosion resistance. Song[19] and Pawar[20] et al indicated that the micro-galvanic corrosion between twins and matrix inevitably occurs and accelerates the dissolution of Mg substrate due to the difference in corrosion resistance of basal planes and prism planes. In addition, the corrosion resistance of the as-extruded AZ31 alloy bar is mainly determined by the micro-galvanic corrosion between different grains (including twinned and un-twinned areas) due to their different crystallographic orientations[16]. Aung et al[17] also revealed that the existence of twins can further accelerate the corrosion of AZ31B alloy, which is ascribed to the high dislocation density caused by the formation of deformed twins.

To eliminate the effect of residual stress (dislocation) on the

Received date: March 23, 2022
Foundation item: National Natural Science Foundation of China (51901047); Guangdong Province Science and Technology Plan Project (2021A1515010660); Guangzhou Science and Technology Plan Project (202102021101)
Corresponding author: Li Chuanqiang, Ph. D., Associate Professor, School of Materials and Energy, Guangdong University of Technology, Guangzhou 510006, P. R. China, E-mail: cqli13s@alum.imr.ac.cn

corrosion of Mg alloys, annealing treatment is usually conducted to decrease the dislocation. In fact, annealing treatment plays an essential role in the growth or suppression of twins in Mg alloys. On the one hand, the reduced back stress arising from dislocation elimination during annealing leads to a decreased repulsive force on twin growth[21–22]. Furthermore, the boundaries of pre-existing deformation twins tend to migrate during annealing. As a result, the twins grow and a merge between the matrix grains and twins occurs[23]. On the other hand, the twin growth is retarded by the pinning effect of solute atoms in twin boundaries during annealing[24–25]. Therefore, the as-extruded binary Mg-Li alloys without solute atoms were used in this research to investigate the effect of twins with a considerable size on the corrosion behavior of magnesium alloy. In general, the deformation twins can hardly form in Mg-Li alloys after hot deformation due to their better deformation ability at high temperatures. However, the annealing twins appear in the matrix during annealing at 200−300 °C[26–29]. It is reported that the as-cast/extruded Mg-4Li alloy after annealing at 300 °C possesses twins. In addition, a large number of lenticular twins are generated in Mg-4Li-1Al alloy after annealing at 250 °C[28–29]. Recently, the annealing twins have been found in traditional as-extruded Mg-Zn-Y-Nd alloy during annealing at 225 and 250 °C with a weak fiber texture[30].

Therefore, the corrosion resistance of Mg-Li alloy with annealing twins was studied and the corresponding mechanisms were discussed. The as-extruded Mg-*x*Li (*x*=1, 3, 5, wt%) alloys with annealing twins were prepared in this study, and their effect on the corrosion resistance was investigated.

1 Experiment

The initial materials were as-extruded Mg-1Li, Mg-3Li, and Mg-5Li (wt%) alloy plates with extrusion ratio of about 6.5 at 300 °C. Then, the specimens were cut from the extruded plates and annealed at 300 °C for 4 h. Afterwards, the specimens were ground by SiC paper (the finest was 5000#) and polished with diamond suspension of 1 μm. Then, the polished specimens were etched by 5vol% nitric acid+95vol% ethanol to observe the grain and twinning structures via optical microscope (OM).

To study the corrosion resistance, the as-extruded and as-annealed Mg-Li alloy specimens with dimension of 12 mm× 10 mm×3 mm were immersed in 0.1 mol/L NaCl solution (pH =6.9) at room temperature for different durations. After immersion, the specimens were cleaned by water and ethanol and then dried. Then the surface was observed by OM. Subsequently, the specimens were further cleaned to remove the corrosion products by chromic acid consisting of 180 g/L CrO_3. Finally, the surface morphologies of the specimens were observed by confocal laser scanning microscope (CLSM, OLYMPUS LEXT OLS4000) and scanning electron microscope (SEM, JEOL JSM-IT100).

Electrochemical tests of potentiodynamic polarization were conducted with scanning rate of 1 mV/s by Wuhan CorrTest electrochemistry test system (CS350H). A classical three-electrode cell with platinum, saturated calomel electrode (SCE), and the specimens with exposure area of 1 cm^2 were used as the counter electrode, reference electrode, and the working electrode, respectively. The measurements were performed in 0.1 mol/L NaCl solution at room temperature. To ensure the reliability, each test was conducted as least three times, and an initial delay of 600 s was set for polarization measurements to provide a relatively stable test system at open circuit potential. Besides, the altitude mapping on the initial corroded surface of as-annealed Mg-3Li specimen was examined by scanning Kelvin probe force microscope (SKPFM, Multimode 3D, Bruker Corporation) in the work function mode.

2 Results and Discussion

2.1 Microstructure and corrosion resistance

The initial microstructures of the as-extruded and as-annealed Mg-*x*Li (*x*=1, 3, 5) alloys are shown in Fig. 1. The twins can hardly be observed in the as-extruded Mg-*x*Li alloys, and the grain size barely changes with increasing the lithium content. Meanwhile, the deformed microstructure is inconspicuous, which is ascribed to the occurrence of recrystallization during hot extrusion[31]. However, after annealing treatment, all the alloys present some annealing twins. Due to the same preparation method for the as-extruded and as-annealed alloy specimens, the twins are generated by the annealing treatment rather than the additive induced by the postprocessing polished surface. Moreover, the residual stress induced by deformation dislocation exists in the wrought magnesium alloy. Once the dislocation annihilation occurs during annealing, the alleviated back stress can decrease the repulsive force on the formation of twins[21–22]. Therefore, the annealing twins emerge in all the Mg-*x*Li alloys after annealing, which is in agreement with the results in Ref.[29].

The mass loss of as-extruded and as-annealed Mg-*x*Li alloys after immersion in 0.1 mol/L NaCl solution for 72 h is shown in Fig. 2. The corrosion morphologies of as-extruded and as-annealed Mg-*x*Li alloys are shown in Fig. 3. It can be seen that the corrosion resistance of as-annealed specimens is worse than that of the as-extruded ones. As for the as-extruded Mg-*x*Li alloys, the corrosion resistance is improved with increasing the lithium content, which is consistent with the results in Ref. [31]. In addition, it is apparent that the as-annealed Mg-1Li alloy is covered by a large amount of corrosion product, implying the worst corrosion resistance. With increasing the lithium content, the corrosion product covered on the surface of as-annealed Mg-3Li and Mg-5Li alloys is reduced gradually, indicating that the more the lithium, the better the corrosion resistance. These phenomena are similar to those of the as-extruded ones. The main mechanism is that the protective film forms on the Mg-Li alloy surface with more Li_2CO_3 compound, i.e., with higher lithium content[32–34]. The deteriorative corrosion resistance of the as-annealed alloy is closely related to the annealing twins. The crystal orientation of twined area is generally different

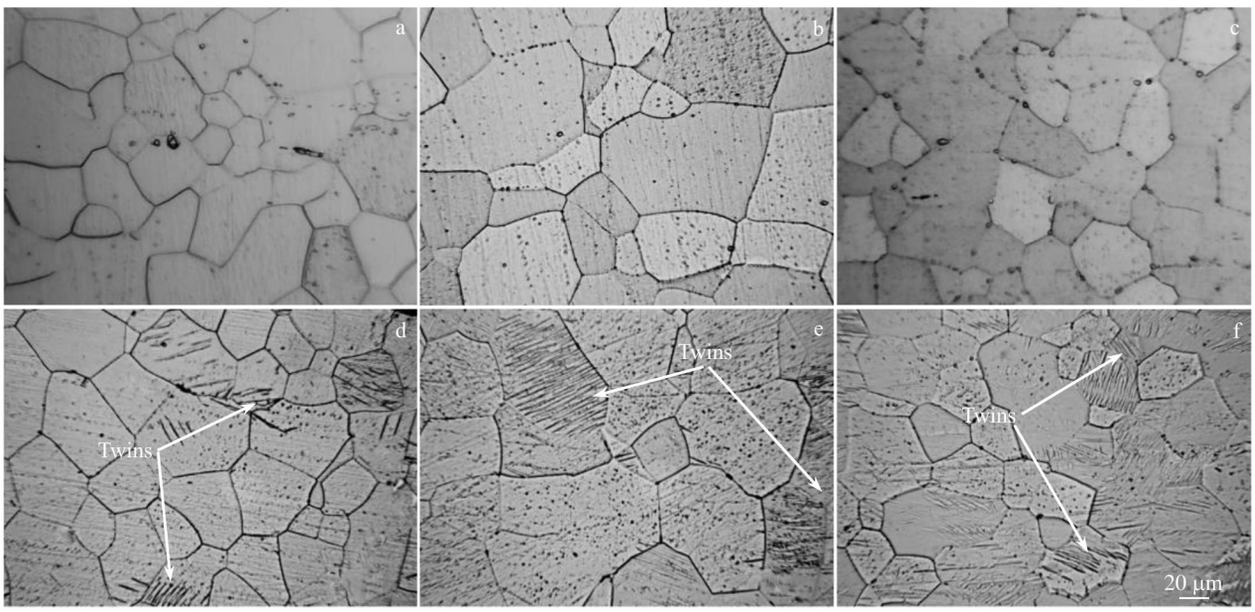

Fig.1 OM microstructures of as-extruded (a–c) and as-annealed (d–f) Mg-*x*Li alloys: (a, d) Mg-1Li alloy, (b, e) Mg-3Li alloy, and (c, f) Mg-5Li alloy

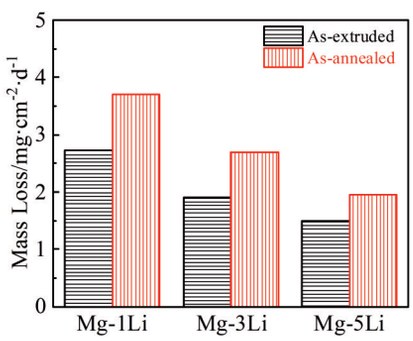

Fig.2 Mass loss of as-extruded and as-annealed Mg-*x*Li alloys after immersion in 0.1 mol/L NaCl solution for 72 h

from that of the parental grains, and the corrosion anisotropy occurs in wrought Mg alloys[16–17,35]. Therefore, compared with the as-extruded alloys, more micro-galvanic couples form in the as-annealed Mg-Li alloys with the annealing twins.

To obtain the instantaneous polarisation response and corresponding reaction kinetics, the potentiodynamic polarization curves of Mg-*x*Li alloys in 0.1 mol/L NaCl solution are shown in Fig. 4. According to the polarisation response of Mg-*x*Li alloys, it is deduced that the cathodic hydrogen evolution reaction (HER) kinetics is gradually increased with the formation of annealing twins in these alloys. The anodic reaction kinetics of as-extruded and as-annealed Mg-*x*Li alloys are similar, i. e., regardless of the annealing treatment, the Mg-Li alloys have similar anodic Tafel slopes and they do not have the passivity region. Therefore, the anodic dissolution and surface film are basically the same for the Mg-*x*Li alloys before and after annealing with the same lithium content. Furthermore, the anodic Tafel slope associated with the anode reaction barely changes after annealing treatment, even though the polarisation curve shifts slightly. Thus, the controlling factor of the corrosion resistance of three alloys is at the point where the cathodic kinetics intersect the anodic one to form the corrosion potential E_{corr}, in terms of corrosion current density. It is also concluded that the corrosion resistance of the three alloys is decreased after annealing treatment due to the formed annealing twins.

2.2 Corrosion morphologies

SEM morphologies of corroded surfaces of as-extruded and as-annealed Mg-1Li alloy after immersion in 0.1 mol/L NaCl solution for different durations are shown in Fig. 5. Typical filiform corrosion occurs in as-extruded Mg-1Li alloy at the initial stage (Fig. 5a), and obvious corrosion pits appear with prolonging the immersion time to 2 h (Fig. 5b). The corrosion pits enlarge gradually, and the corrosion filaments remain on the alloy surface when the immersion time increases to 16 h (Fig. 5c). No corrosion filament can be observed in the as-annealed Mg-1Li alloy after immersion for 1 h. The corrosion becomes severe and the corrosion pits are apparent in as-annealed Mg-1Li alloy after immersion for 2 and 16 h, indicating the worse corrosion resistance of the as-annealed specimen, compared with that of the as-extruded one. The longer the immersion time, the more the corrosion pits, and the more severe the corrosion damage of surface. Therefore, it is suggested that the annealing twins accelerate the corrosion of as-annealed Mg-1Li alloy. Similar corrosion characterization can be observed in Mg-3Li and Mg-5Li alloys, as shown in Fig. 6 and Fig. 7, respectively. It is worth noting that the corrosion damage, including corroded surface and corrosion pits, is reduced slightly with increasing the lithium content. Therefore, the electrochemical condition is obstructed by the redistribution of corrosion current on the

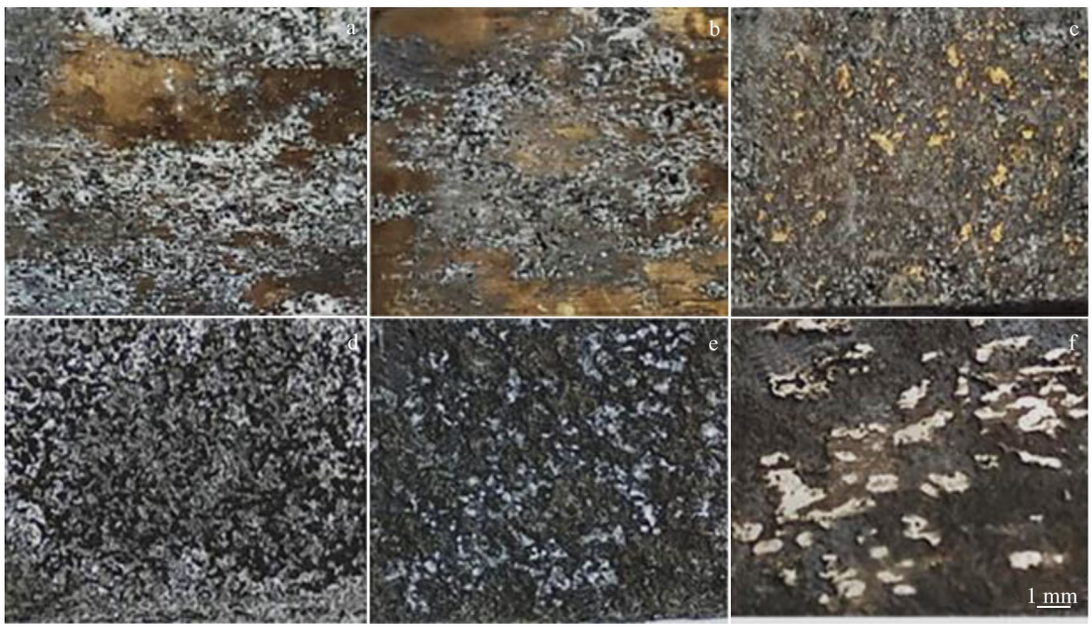

Fig.3 Corrosion morphologies of as-extruded (a–c) and as-annealed (d–f) Mg-*x*Li alloys after immersion in 0.1 mol/L NaCl solution for 48 h: (a, d) Mg-1Li alloy, (b, e) Mg-3Li alloy, and (c, f) Mg-5Li alloy

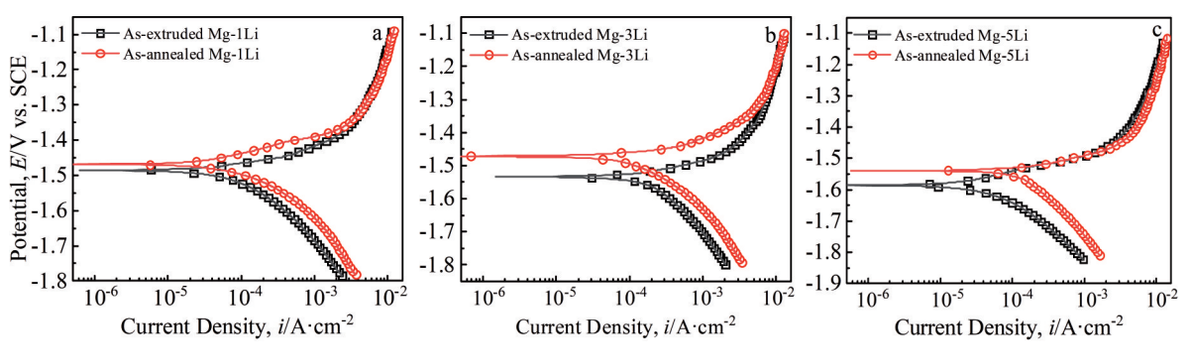

Fig.4 Potentiodynamic polarization curves of as-extruded and as-annealed Mg-1Li alloy (a), Mg-3Li alloy (b), and Mg-5Li alloy (c) in 0.1 mol/L NaCl solution

alloy surface due to the existence of micro-galvanic corrosion between annealing twins and parental grains in as-annealed alloys, which facilitates the formation of filiform corrosion. Meanwhile, the micro-galvanic effect plays a negative role in the corrosion behavior of hcp binary Mg-Li alloys with annealing twins. In general, the filiform corrosion consists of an intense anode propagation front, which is supported by a cathodically activated filament. Thus, the net cathode on the locally corroded regions is galvanically coupled with the adjacent intense anode regions to drive the lateral propagation of the corrosion product across the exposed surface[36–37]. Besides, the filiform corrosion is a particular form of tunneling, which is the forerunner of regular pitting. In addition, the filiform propagation is promoted by hydrogen evolution during corrosion[38]. Therefore, the annealing twins alter the distribution of corrosion potential for filiform corrosion, resulting in a different corrosion form for the alloys. Moreover, the corrosion filaments randomly form in the as-extruded alloys due to the absence of micro-galvanic effect between twins and matrix grains. However, the path of corrosion filaments can be hindered by the annealing twins and the micro-galvanic effect, resulting in the disappearance of filiform corrosion (pitting corrosion at early stage) in the as-annealed alloys.

Typical 3D CLSM images of corroded as-annealed Mg-*x*Li (*x*=1, 3, 5) alloys are shown in Fig. 8, which illustrates the effect of annealing twins on the depth of corrosion pits after immersion in 0.1 mol/L NaCl solution for different durations. The maximum depth of corrosion pits in as-extruded Mg-1Li alloy is increased from 344 μm to 460 μm with prolonging the immersion duration from 1 h to 4 h, and it is continuously increased to 680 μm after immersion for 16 h. As for the as-annealed Mg-3Li alloys, the depth of corrosion pits is 229, 327, and 599 μm when the immersion duration is 1, 4, and 16 h, respectively, presenting the similar tend to that of as-annealed Mg-1Li alloy. However, the depth of corrosion pits

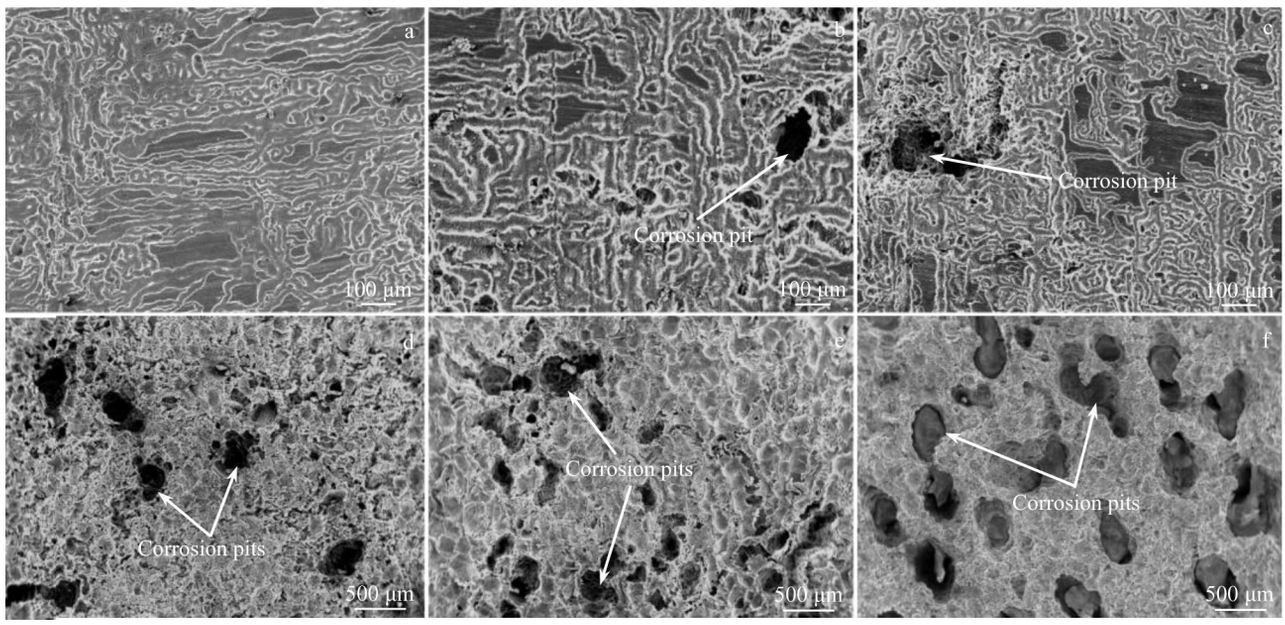

Fig.5 SEM morphologies of as-extruded (a–c) and as-annealed (d–f) Mg-1Li alloys after immersion in 0.1 mol/L NaCl solution for different durations and removal of corrosion product: (a, d) 1 h, (b, e) 2 h, and (c, f) 16 h

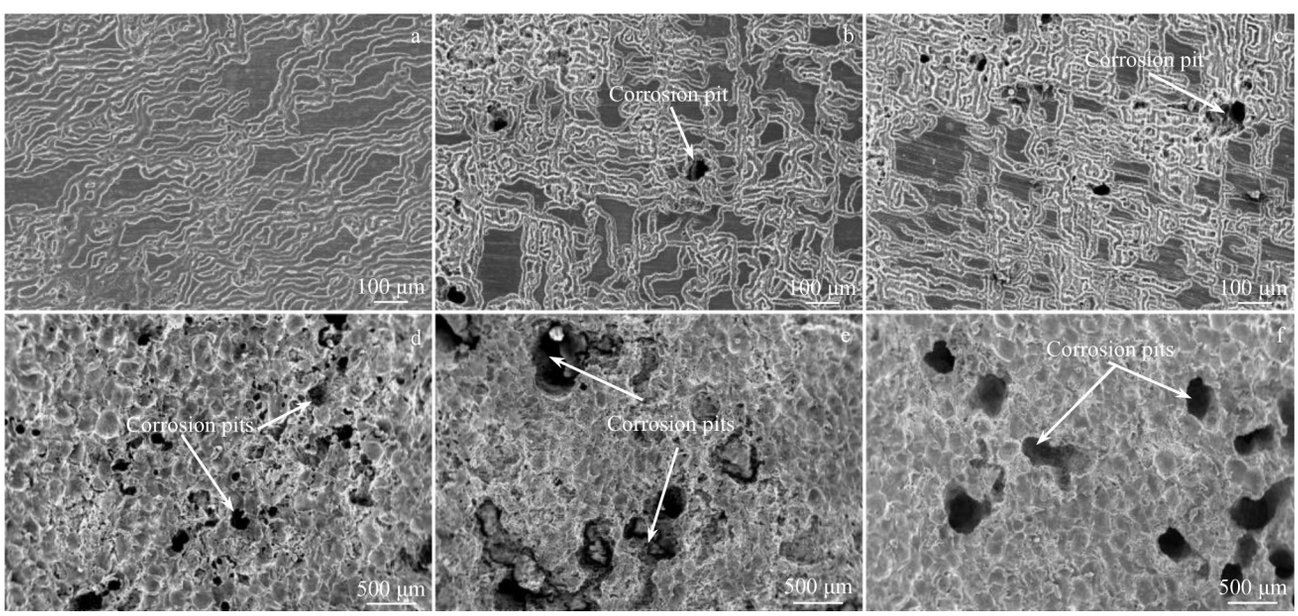

Fig.6 SEM morphologies of as-extruded (a–c) and as-annealed (d–f) Mg-3Li alloys after immersion in 0.1 mol/L NaCl solution for different durations and removal of corrosion product: (a, d) 1 h, (b, e) 2 h, and (c, f) 16 h

of as-annealed Mg-3Li alloy is decreased after immersion for the same duration, compared with that of the as-annealed Mg-1Li alloy. When the lithium content increases to 5wt%, the depth of corrosion pits is the smallest after immersion for the same duration: the depth of corrosion pits is 193, 281, and 424 μm after immersion for 1, 4, and 16 h, respectively. The 3D CLSM images of as-extruded Mg-*x*Li (*x*=1, 3, 5) alloys are shown in Ref.[31]. Thus, the as-annealed Mg-Li alloys exhibit deeper corrosion pits than the as-extruded alloys do after immersion for the same duration, which agrees well with the SEM morphologies and electrochemical test results. The initial corrosion surface of Mg-3Li alloy polished and etched by 5vol% nitric acid+95vol% ethanol for 20 s was observed via SKPFM, and the altitude mapping of the corroded surface is shown in Fig. 9. It can be seen that the shaded annealing twins and the bright parental grains are distributed in the altitude mapping, indicating that the annealing twins are preferentially deteriorated due to their low-altitude location. Therefore, the micro-galvanic corrosion between the twining and untwining areas occurs in as-annealed alloys, leading to the rapid dissolution of anodic annealing twins. Consequently, the corrosion resistance of as-annealed alloys subjected to

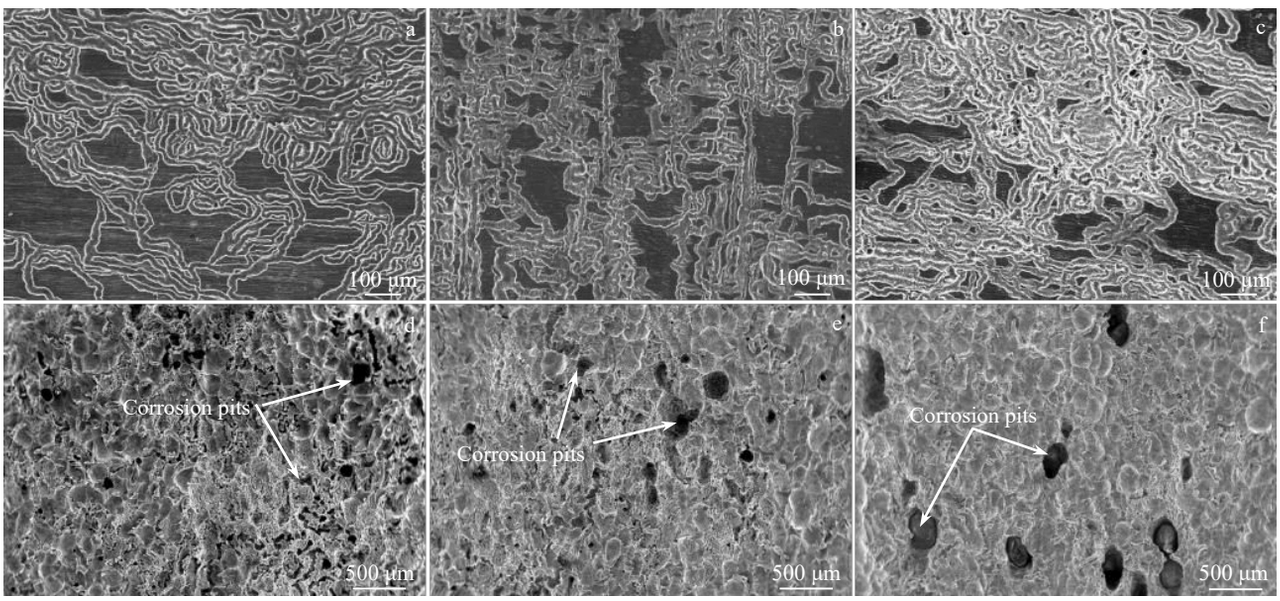

Fig.7 SEM morphologies of as-extruded (a–c) and as-annealed (d–f) Mg-5Li alloys after immersion in 0.1 mol/L NaCl solution for different durations and removal of corrosion product: (a, d) 1 h, (b, e) 2 h, and (c, f) 16 h

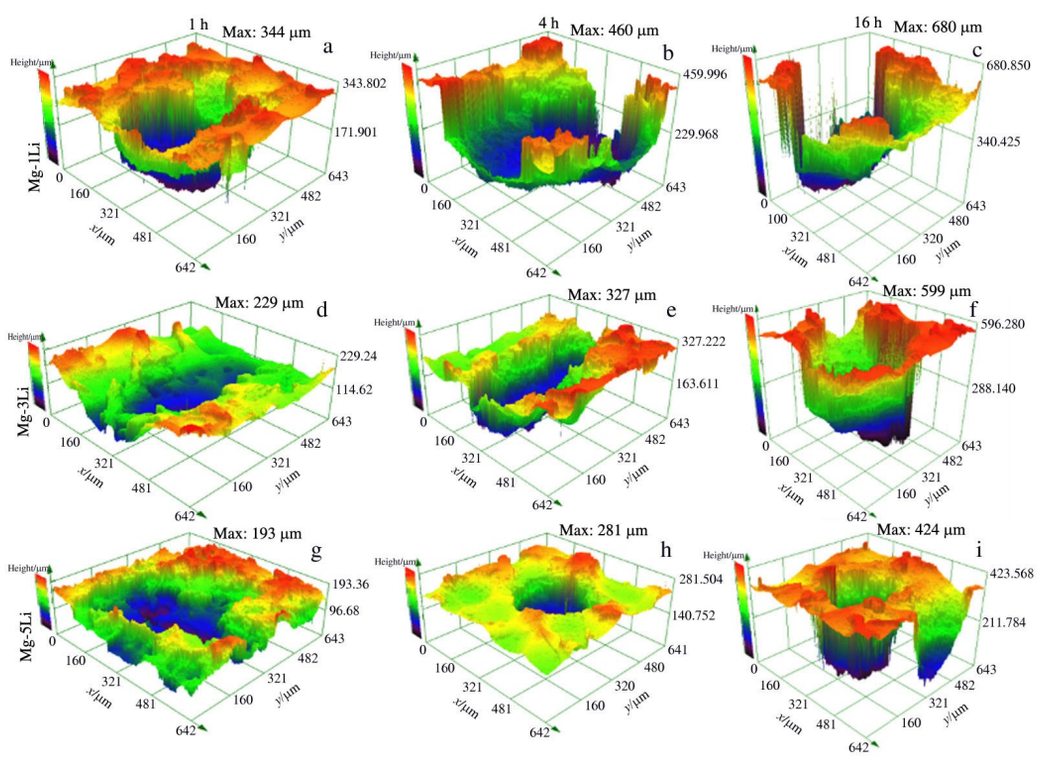

Fig.8 3D CLSM images of as-annealed Mg-1Li alloy (a–c), Mg-3Li alloy (d–f), and Mg-5Li alloy (g–i) after immersion in 0.1 mol/L NaCl solution for 1 h (a, d, g), 4 h (b, e, h), and 16 h (c, f, i)

micro-galvanic corrosion is inferior to that of the as-extruded alloys without annealing twins.

2.3 Discussion

In general, the corrosion anisotropy occurs in the deformed magnesium alloy due to the crystallographic texture. Wang et al[16] reported that the alloy surface with a high concentration of {1010} and {1120} oriented prism planes is more electrochemically stable and shows better corrosion resistance, compared with the alloy surface with a high concentration of {0002}, {1010}, and {1120} oriented planes. Besides, the $\{10\bar{1}0\}/\{11\bar{2}0\}$ orientated grains are preferentially attacked during the corrosion process, compared with the {0002} orientated grains[39]. Different corrosion performances of these crystallographic planes can be

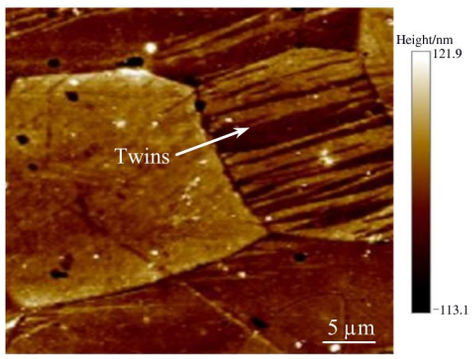

Fig.9 SKPFM altitude mapping of corroded surface of as-annealed Mg-3Li alloy after corrosion by 5vol% nitric acid+95vol% ethanol for 20 s

ascribed to their different anodic and cathodic reaction activities. Ref. [31] reported the existence of (0002) basal texture in the as-extruded plates[31], indicating that more corrosion-resistant (0002) oriented planes exist in the alloy. Therefore, a weak micro-galvanic effect occurs between planes of different orientations in the as-extruded alloys. The schematic diagram of corrosion mechanism of Mg-Li alloys in NaCl solution is shown in Fig.10a.

Twinning is a common dislocation mode in the magnesium alloys, and the misorientation angle between the twins and parental grains is general about 86° and 56° for the $\{10\bar{1}2\}$ tension twins and $\{10\bar{1}1\}$ compression twins[40], respectively. Based on the orientation mapping of grains for the as-extruded Mg-Li alloys[31], much more basal (0002) planes with high

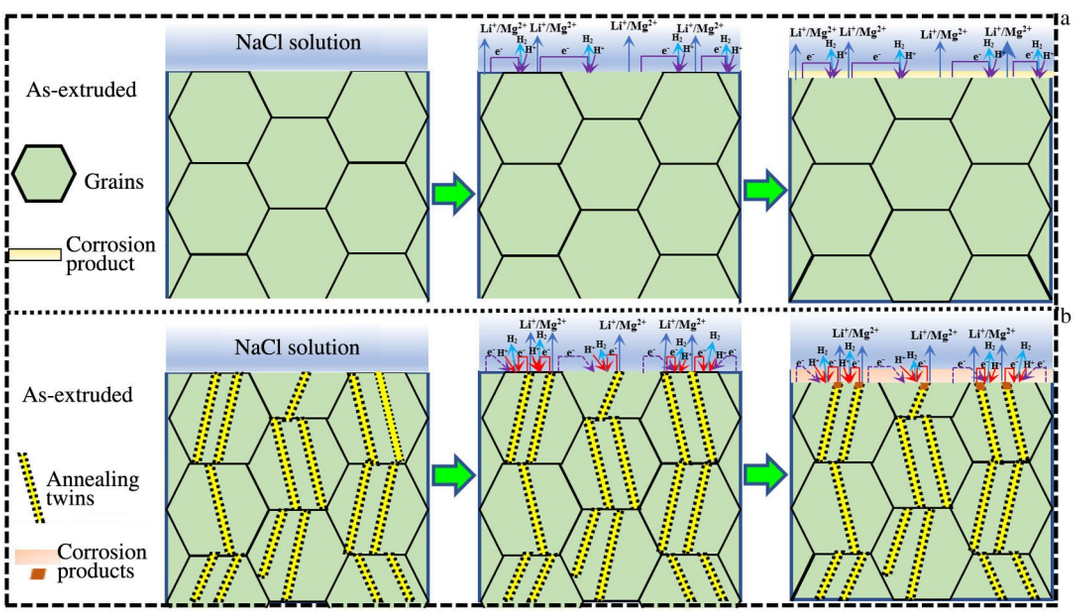

Fig.10 Schematic diagrams of corrosion mechanism for as-extruded (a) and as-annealed (b) hcp binary Mg-Li alloys

corrosion resistance are exposed on the alloy surface. However, much more non-basal oriented planes induced by the annealing twins are exposed on the alloy surface in this research, resulting in the rapid dissolution of non-basal oriented planes without corrosion resistance. Furthermore, Wang et al[16] reported that the corrosion resistance of as-extruded AZ31 magnesium alloy bar is mainly determined by the galvanic corrosion between the grains and between the twinned and un-twinned areas due to their different crystallographic orientations. Thus, new corrosion cells can form between the twin areas and parental grains in the as-annealed alloys (Fig. 10b). Moreover, the residual stress from the deformation dislocation of wrought magnesium alloy deteriorates the corrosion resistance. However, the alleviated residual stress induced by the dislocation annihilation during annealing can decrease corrosion degradation[41]. Therefore, the as-annealed Mg-Li alloys with eliminated residual stress exhibit an apparently inferior corrosion resistance, compared with the as-extruded Mg-Li alloys with inevitable residual stress, which further confirms the adverse effect of annealing twins on the corrosion resistance of Mg-Li alloys.

3 Conclusions

1) Annealing twins form in the as-extruded binary Mg-*x*Li (*x*=1, 3, 5, wt%) alloys after annealing at 350 °C for 4 h.

2) The corrosion resistance of both as-annealed and as-extruded Mg-Li alloys in 0.1 mol/L NaCl solution is improved with increasing the lithium content.

3) Due to the micro-galvanic corrosion between the annealing twins and parental grains, the as-annealed Mg-Li alloys with annealing twins present a worse corrosion resistance.

References

1 Edwin E K, Jiang J H, Bassiouny S *et al*. *Rare Metal Materials*

and Engineering[J], 2022, 51(2): 491
2 Estrin Y, Nene S S, Kashyap B P *et al*. *Materials Letters*[J], 2016, 173: 252
3 Wu R, Yan Y, Wang G *et al*. *International Materials Reviews*[J], 2015, 60(2): 65
4 Park G H, Kim J T, Park H J *et al*. *Journal of Alloys and Compounds*[J], 2016, 680: 116
5 Li C Q, Deng B B, Dong L J *et al*. *Journal of Alloys and Compounds*[J], 2022, 895: 162 718
6 Liu Yuxiang. *Rare Metal Materials and Engineering*[J], 2021, 50(1): 361 (in Chinese)
7 Li C Q, Xu D K, Wang B J *et al*. *Journal of Materials Science and Technology*[J], 2019, 35: 2477
8 Li C Q, Xu D K, Yu S *et al*. *Journal of Materials Science and Technology*[J], 2017, 33(5): 475
9 Mineta T, Hasegawa K, Sato H. *Materials Science and Engineering A*[J], 2020, 773: 138 867
10 Chen X Y, Zhang Y, Cong M Q *et al*. *Transactions of Nonferrous Metals Society of China*[J], 2020, 30(8): 2079
11 Shi H N, He J G, Wen J B *et al*. *Rare Metal Materials and Engineering*[J], 2021, 50(11): 3871
12 Liu T T, Yang Q S, Guo N *et al*. *Journal of Magnesium and Alloys*[J], 2020, 8(1): 66
13 Nayeb-Hashemi A A, Clark J B. *Bulletin of Alloy Phase Diagrams*[J], 1984, 5(5): 365
14 Zou G D, Peng Q M, Wang Y N *et al*. *Journal of Alloys and Compounds*[J], 2015, 618: 44
15 Liu J H, Han E H, Song Y W *et al*. *Journal of Alloys and Compounds*[J], 2018, 757: 356
16 Wang B J, Xu D K, Dong J H *et al*. *Scripta Materialia*[J], 2014, 88: 5
17 Aung N N, Zhou W. *Corrosion Science*[J], 2010, 52(5): 589
18 Peng J H, Zhang Z, Long C *et al*. J*ournal of Alloys and Compounds*[J], 2020, 827: 154 096
19 Song G L, Xu Z. *Corrosion Science*[J], 2012, 63: 100
20 Pawar S, Slater T J A, Burnett T L *et al*. *Acta Materialia*[J], 2017, 133: 90
21 Liu S, Zhang J, Xi G Q *et al*. *Journal of Alloys and Compounds*[J], 2018, 763: 11
22 Cui Y J, Li Y P, Wang Z C *et al*. *International Journal of Plasticity*[J], 2017, 99: 1
23 Zhao L Y, Yan H, Chen R S *et al*. *Materials Characterization*[J], 2020, 170: 110 697
24 Chen J, Wang Z Q, Ma X G *et al*. *Journal of Alloys and Compounds*[J], 2015, 642: 92
25 Nie J F, Zhu Y M, Liu J Z *et al*. *Science*[J], 2013, 340(6135): 957
26 Li C Q, Xu D K, Wang B J *et al*. *Journal of Materials Science and Technology*[J], 2016, 32(12): 1232
27 Cao F R, Zhou B J, Yin B *et al*. *Transactions of Nonferrous Metals Society of China*[J], 2017, 27(11): 2434
28 Bhagat S P, Sabat R K, Kumaran S *et al*. *Journal of Materials Engineering and Performance*[J], 2018, 27(2): 864
29 Wang C, Xu Y B, Han E H. *Journal of Metallurgy*[J], 2012: 674 573
30 Sheng L Y, Du B N, Hu Z Y *et al*. *Journal of Magnesium and Alloys*[J], 2020, 8(3): 601
31 Li C Q, He Y B, Huang H P. *Journal of Magnesium and Alloys*[J], 2021, 9(2): 569
32 Li C Q, Tong Z P, He Y B *et al*. *Transactions of Nonferrous Metals Society of China*[J], 2020, 30(9): 2413
33 Li C Q, Xu D K, Chen X B *et al*. *Electrochimica Acta*[J], 2018, 260: 55
34 Xu W Q, Birbilis N, Sha G *et al*. *Nature Materials*[J], 2015, 14(12): 1229
35 Wang B J, Xu D K, Cai X *et al*. *Journal of Magnesium and Alloys*[J], 2021, 9(2): 560
36 Williams G, Birbilis N, McMurray N H. *Faraday Discuss*[J], 2015, 180: 313
37 Cano Z P, McDermid J R, Kish J R. *Journal of the Electrochemical Society*[J], 2015, 162(14): C732
38 Ghali E, Dietzel W, Kainer K. *Journal of Materials Engineering and Performance*[J], 2004, 13(1): 7
39 Yang H B, Wu L, Jiang B *et al*. *Journal of Materials Science and Technology*[J], 2021, 62: 128
40 Song Guangsheng, Zhang Jianqiang, Zhang Shihong. *Rare Metal Materials and Engineering*[J], 2020, 49(1): 288 (in Chinese)
41 Ma L N, Yang Y, Zhou G *et al*. *Transactions of Nonferrous Metals Society of China*[J], 2020, 30(7): 1816

退火孪晶对hcp结构二元镁锂合金腐蚀行为的影响

刘　茜，邓斌斌，李传强
(广东工业大学 材料与能源学院，广东 广州 510006)

摘　要：采用浸泡实验、电化学实验、腐蚀形貌观察以及扫描开尔文探针测试等实验方法对挤压态和退火态二元Mg-*x*Li（*x*=1，3，5，质量分数，%）合金的耐腐蚀性能进行研究。结果表明：挤压态Mg-Li合金经350 ℃/4 h退火处理后，可在基体中形成退火孪晶。在0.1 mol/L NaCl溶液中，退火态合金的耐腐蚀性能明显劣于挤压态合金。通过扫描电子显微镜和激光共聚焦三维形貌分析，发现挤压态合金在腐蚀初期具有丝状腐蚀特征，并且随着腐蚀时间的延长形成了腐蚀坑；退火态合金表面发生快速腐蚀损伤，同时形成较大且深的腐蚀坑形貌。另外，退火态Mg-3Li合金的腐蚀等势线分布表明该合金退火孪晶区域优先发生了腐蚀溶解现象。因此，退火孪晶与母体晶粒之间可形成微电偶腐蚀效应，且退火孪晶区域充当阳极，母体晶粒作为阴极，从而降低了退火态Mg-Li合金的耐腐蚀性能。

关键词：Mg-Li合金；退火孪晶；腐蚀；电化学；微电偶

作者简介：刘　茜，女，1998年生，硕士，广东工业大学材料与能源学院，广东 广州 510006，E-mail：1738773905@qq.com